Overcrowding Motifs in Large PAHs. An ab Initio Study

Sergey Pogodin and Israel Agranat*

Department of Organic Chemistry, The Hebrew University of Jerusalem, Jerusalem 91904, Israel

isria@vms.huji.ac.il

Received July 17, 2001

Planar and overcrowded LPAHs $C_{34}H_{18}$ anthra[9,1,2-*cde*]benzo[*rst*]penaphene (**1**), benzo[*rst*]-phenanthro[10,1,2-*cde*]pentaphene (**2**), tetrabenzo[*a*,*cd*,*j*,*lm*]perylene (**3**), tetrabenzo[*a*,*cd*,*lm*,*o*]-perylene (**4**), and LPAHs $C_{38}H_{18}$ anthra[2,1,9,8-*klmno*]naphtho[3,2,1,8,7-*vwxyz*]hexaphene (**5**), dianthra[2,1,9,8-*stuva*;2′,1′,9′,8′-*hijkl*]pentacene (**6**), dibenzo[*jk*,*uv*]dinaphtho[2,1,8,7-*defg*;2′,1′,8′,7′-*opqr*]perylene (**7**), diphenanthro[5,4,3-*abcd*;3′,4′,5′-*lmno*]perylene (**8**), potential products of *peri*-*peri* reductive couplings of benzanthrone and of naphthanthrone, respectively, were subjected to an ab initio study with emphasis on overcrowding motifs. The HF and DFT B3LYP methods were employed to calculate energies and geometries of the minima conformations of these LPAHs. The most stable LPAHs in these series were found to be planar C_{2v}-**1** and C_{2v}-**5**, respectively. Among overcrowded LPAHs, twisted-folded C_2-**3** and C_2-**7** with two cove regions were found to be more stable than their respective isomers twisted-folded C_2-**4** and C_2-**8** with one fjord region each, in contrast to the semiempirical predictions. The energy differences between the most stable planar isomer and the overcrowded isomers were significantly smaller in the $C_{38}H_{18}$ series, than in the $C_{34}H_{18}$ series. Overcrowded twisted-folded C_2-**7** with two coves was found to be more stable than planar C_{2h}-**6** by 2.0 kJ/mol (at B3LYP/6-311G**), indicating enhanced role of aromatic stabilization and decreased destabilization due to overcrowding, with increasing the number of aromatic rings. Heats of formation of LPAHs **1**−**8** were derived from the ab initio total energies (at B3LYP/6-31G*). A search of the conformational spaces of **3** and **4** revealed an *anti*-folded local minimum C_i-**3** and a *syn*-folded transition state C_s-**4**, 23.7 and 120.3 kJ/mol higher in energy than the twisted-folded C_2-**3** and C_2-**4**, respectively (at B3LYP/6-31G*). The cove and fjord torsion angles in the $C_{38}H_{18}$ series were found to be smaller than in the $C_{34}H_{18}$ series. The nonbonding distances between carbon atoms at cove and fjord regions of the overcrowded LPAHs were found to be smaller than the sum of the van der Waals radii of two carbon atoms

Introduction

Large polycyclic aromatic hydrocarbons (LPAHs), namely heptacyclic and higher PAHs, are ubiquitous, from the bottom of the oceans to the dust clouds of interstellar space.[1,2] Herndon has shown that the majority of PAHs must adopt nonplanar conformations as global minima.[3] The nonplanarity is especially frequent in LPAHs. The abundance of overcrowded LPAHs results in a predominance of chiral LPAHs. The most important overcrowding motifs in PAHs are bay, cove, and fjord.[4] These motifs play a significant role in the mechanisms of carcinogenesis of PAHs, e.g., the bay-region diol epoxide theory.[5] Dibenzo[*a*,*l*]pyrene (DB[*al*]P),[6,7] one of the worst environmental hazards,[8,9] has a cove region and is chiral, while the notorious carcinogen benzo[*a*]pyrene (B[*a*]P)[10] has a bay region and is planar.[11] LPAHs have recently attracted considerable attention not only as environmental contaminants, but also as coal hydrogenation byproducts[12] and as precursors to fullerenes.[13−15] The earlier expectation that no significant biological impact would result from exposure to LPAHs, which were

(1) Allamandola, L. J. *Top. Curr. Chem.* **1990**, *153*, 1−26.
(2) Biggs, W. R.; Fetzer, J. C. *Trends Anal. Chem.* **1996**, *15*, 196−206.
(3) (a) Herndon, W. C.; Connor, D. A.; Lin, P. *Pure Appl. Chem.* **1990**, *62*, 435−444. (b) Herndon, W. C.; Nowak, P. C.; Connor, D. A.; Lin, P. *J. Am. Chem. Soc.* **1992**, *114*, 41−47. (c) Herndon, W. C.; Nowak, P. C. In *Advances in Theoretically Interesting Molecules*; Thummel, R. P. Ed.; JAI Press: Greenwich, CT, 1992; Vol. 2, pp 113−144.
(4) Cove and fjord are the overcrowded regions in benzo[*c*]phenanthrene ([4]helicene) and dibenzo[*c*,*g*]phenanthrene ([5]helicene), respectively: Gutman, I.; Cyvin, S. J. *Introduction to the Theory of Benzenoid Hydrocarbons*; Springer-Verlag: Berlin, 1989; pp 21−22.
(5) (a) Lehr, R. E.; Kumar, S.; Levin, W.; Wood, A. W.; Chang, R. L.; Conney, A. H.; Yagi, H.; Sayer, J. M.; Jerina, D. M. In *Polycyclic Hydrocarbons and Carcinogenesis*, ACS Symposium Series 283; Harvey, R. G. Ed.; American Chemical Society: Washington D. C., 1985; pp 63−84. (b) Wislocki, P. G.; Lu, A. Y. H. In *Polycyclic Aromatic Hydrocarbon Carcinogenesis: Structure−Activity Relationships*; Yang, S. K.; Silverman, B. D., Eds.; CRC Press: Boca Nova, FL, 1988; pp 1−27. (c) Harvey, R. G. *Polycyclic Aromatic Hydrocarbons: Chemistry and Carcinogenicity*; Cambridge University Press: Cambridge, U.K., 1991; pp 50−95.
(6) Katz, A. K.; Carrell, H. L.; Glusker, J. P. *Carcinogenesis* **1998**, *19*, 1641−1648.
(7) Ralston, S. L.; Coffing, S. L.; Seidel, A.; Luch, A.; Platt, K.-L.; Baird, W. M. *Chem. Res. Toxicol.* **1997**, *10*, 687−693.
(8) Jacob, J. *Pure Appl. Chem.* **1996**, *68*, 301−308.
(9) Cavalieri, E. L.; Rogan, E. G.; Higginbothan, S.; Cremonesi, P.; Salmasi, S. *J. Cancer Res. Clin. Oncol.* **1989**, *115*, 67.
(10) Iball, J.; Scrimgeour, S. N.; Young, D. W. *Acta Crystallogr. B* **1976**, *B32*, 328−330.
(11) Osborne, M. R.; Crosby, N. T. *Benzopyrenes*; Cambridge University Press: Cambridge, U.K., 1987.
(12) Fetzer, J. C.; Biggs, W. R. *Polycyclic Aromat. Compd.* **1994**, *4*, 3−17.
(13) (a) Mehta, G.; Rao, H. S. P. *Advances in Strain in Organic Chemistry*; Halton, B. Ed.; JAI Press: London, 1997; Vol. 6, pp 139−187. (b) Mehta, G.; Rao, H. S. P. *Tetrahedron* **1998**, *54*, 13325−13370.
(14) Rabideau, P. W.; Sygula, A. *Advances in Theoretically Interesting Molecules*; Thummel, R. P. Ed.; JAI Press: Greenwich, CT, 1995; Vol. 3, p 1.
(15) (a) Scott, L. T. *Pure Appl. Chem.* **1996**, *68*, 291−300. (b) Scott, L. T.; Bronstein, H. E.; Preda, D. V.; Ansems, R. B. M.; Bratcher, M. S.; Hagen, S. *Pure Appl. Chem.* **1999**, *71*, 209−219.

10.1021/jo0107251 CCC: $22.00
Published on Web 12/06/2001

assumed to be sparingly soluble and therefore not environmentally relevant has been questioned.[16]

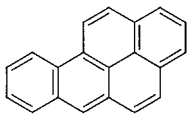

B[*a*]P

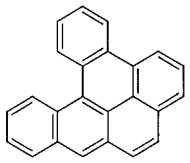

DB[*al*]P

A recent semiempirical AM1 and PM3 study of a series of planar and overcrowded $C_{34}H_{18}$ and $C_{38}H_{18}$ LPAHs has indicated the energetic preference of overcrowded LPAHs with a fjord, as compared with the corresponding isomeric LPAHs with two coves.[17] The shortcomings of the AM1 and PM3 methods have previously been reflected in their predictions of heats of formation of simple PAHs,[3b,18] of enantiomerization barriers of nonplanar PAHs[19] and bowl-shaped fullerene fragments,[20] and of conformational energies of overcrowded polycyclic aromatic enes.[21,22] The reliability of the semiempirical results may be questioned also in view of their predictions that overcrowded isomers in the $C_{38}H_{18}$ series were significantly more stable than their corresponding planar isomers.[17] Density functional theory (DFT) based methods are capable of generating a variety of molecular properties, including electronic properties and geometries, quite accurately.[23] It has been known that computational DFT can be used to probe the aromaticity of large molecular systems, in a cost-effective way, using the different energetic, geometrical, and magnetic criteria of aromaticity.[23] A comparative study of experimental and calculated geometries of overcrowded PAHs (and their metabolites), using semiempirical and ab initio Hartree−Fock and DFT methods, has recently been described.[24] We report here the results of an ab initio HF and DFT study of a series of *peri*-condensed overcrowded $C_{34}H_{18}$ and $C_{38}H_{18}$ LPAHs with special emphasis on overcrowding motifs and their destabilizing effects.

Methods

The programs Gaussian94[25] and Gaussian98[26] were used for ab initio Hartree−Fock and DFT calculations. Becke's three parameter hybrid density functional, B3LYP,[27] with the nonlocal correlation functional of Lee, Yang, and Parr,[28,29,30] was used. The basis sets STO-3G, 6-31G*, and, in the case of B3LYP, also 6-311G** were employed. Semiempirical AM1 and PM3 results have previously been published.[17] All structures were fully optimized using symmetry constraints as indicated. Frequencies were calculated to verify minima and higher order saddle points for the B3LYP/STO-3G optimized conformations of the systems under study.

Results and Discussion

The $C_{34}H_{18}$ **1**−**4** and $C_{38}H_{18}$ **5**−**8** LPAHs[31] were subjected to ab initio HF and DFT B3LYP calculations. B3LYP calculations have previously proved to be reliable in calculating fullerene fragments,[20] PCBs,[32] simple PAHs,[18] and coronene and related PAHs.[33] Ab initio DFT calculations of peropyrene (**9**), the parent LPAH of this series, have recently been reported.[34] LPAHs **1**−**8** were selected from a wealth of the potential products (twelve $C_{34}H_{18}$ and six $C_{38}H_{18}$ LPAHs) of *peri-peri* reductive coupling reactions of benzanthrone and of naphthanthrone, respectively.[34,35] This selected subset represents planar as well as overcrowded conformations with cove and fjord regions.

Table 1 gives the ab initio HF/6-31G* and B3LYP/6-31G* relative energies, semiempirical AM1 relative enthalpies of formation (taken from the previous work[17]), selected semiempirical enthalpies of formation and ab initio total energies, ab initio enthalpies of formation (vide infra), symmetries and types of conformations of the optimized structures of **1**−**8** as well as the numbers of Kekulé structures (*K*) of the above LPAHs (the ab initio HF/STO-3G, HF/6-31G*, B3LYP/STO-3G, B3LYP/6-31G*, and B3LYP/6-311G** total and relative energies and semiempirical AM1 and PM3 enthalpies of formation and relative enthalpies of formation are provided in Tables S1 and S2 of the Supporting Information). The following designators of types of conformations are used: **tf**: twisted-folded; **a**: *anti*-folded, **s**: *syn*-folded; **ft**: folded-twisted, **pl**: planar. In the cases where two

(16) Harvey, R. G.; Yang, D. T. C.; Yang, C. *Polycyclic Aromat. Compd*. **1994**, *4*, 127−133.
(17) Pogodin, S.; Agranat, I. *Polycyclic Aromat. Compd*. **2001**, *18*, 247−263.
(18) Herndon, W. C.; Biedermann, P. U.; Agranat, I. *J. Org. Chem*. **1998**, *63*, 7445−7448.
(19) Janke, R. H.; Haufe, G.; Würthwein, E.-U.; Borkent, J. H. *J. Am. Chem. Soc.* **1996**, *118*, 6031−6035.
(20) Biedermann, P. U.; Pogodin, S.; Agranat, I. *J. Org. Chem*. **1999**, *64*, 3655−3662.
(21) Biedermann, P. U.; Stezowski, J. J.; Agranat, I. *Eur. J. Org. Chem*. **2001**, 15−34.
(22) Biedermann, P. U.; Stezowski, J. J.; Agranat, I. *Chem. Commun*. **2001**, 954−955.
(23) De Proft, F.; Geerlings, P. *Chem. Rev*. **2001**, *101*, 1451−1464.
(24) Little, S. B.; Rabinowitz, J. R.; Wei, P.; Yang, W. *Polycyclic Aromat. Compd*. **1999**, *14*−*15*, 53−61.
(25) Frisch, M. J.; Trucks, G. W.; Schlegel, H. B.; Gill, P. M. W.; Johnson, B. G.; Robb, M. A.; Cheeseman, J. R.; Keith, T.; Petersson, G. A.; Montgomery, J. A.; Raghavachari, K.; Al-Laham, M. A.; Zakrzewski, V. G.; Ortiz, J. V.; Foresman, J. B.; Cioslowski, J.; Stefanov, B. B.; Nanayakkara, A.; Challacombe, M.; Peng, C. Y.; Ayala, P. Y.; Chen, W.; Wong, M. W.; Andres, J. L.; Replogle, E. S.; Gomperts, R.; Martin, R. L.; Fox, D. J.; Binkley, J. S.; Defrees, D. J.; Baker, J.; Stewart, J. P.; Head-Gordon, M.; Gonzalez, C.; Pople, J. A. Gaussian 94, Revision E.2, 1995; Gaussian, Inc.: Pittsburgh, PA.
(26) Frisch, M. J.; Trucks, G. W.; Schlegel, H. B.; Scuseria, G. E.; Robb, M. A.; Cheeseman, J. R.; Zakrzewski, V. G.; Montgomery, J. A., Jr.; Stratmann, R. E.; Burant, J. C.; Dapprich, S.; Millam, J. M.; Daniels, A. D.; Kudin, K. N.; Strain, M. C.; Farkas, O.; Tomasi, J.; Barone, V.; Cossi, M.; Cammi, R.; Mennucci, B.; Pomelli, C.; Adamo, C.; Clifford, S.; Ochterski, J.; Petersson, G. A.; Ayala, P. Y.; Cui, Q.; Morokuma, K.; Malick, D. K.; Rabuck, A. D.; Raghavachari, K.; Foresman, J. B.; Cioslowski, J.; Ortiz, J. V.; Baboul, A. G.; Stefanov, B. B.; Liu, G.; Liashenko, A.; Piskorz, P.; Komaromi, I.; Gomperts, R.; Martin, R. L.; Fox, D. J.; Keith, T.; Al-Laham, M. A.; Peng, C. Y.; Nanayakkara, A.; Gonzalez, C.; Challacombe, M.; Gill, P. M. W.; Johnson, B.; Chen, W.; Wong, M. W.; Andres, J. L.; Gonzalez, C.; Head-Gordon, M.; Replogle, E. S.; Pople, J. A. Gaussian 98, Revision A.7, Gaussian, Inc., Pittsburgh, PA, 1998.
(27) Becke, A. D. *J. Chem. Phys*. **1993**, *98*, 5648−5651.
(28) Lee, C.; Yang, W.; Parr, R. G. *Phys. Rev. B* **1988**, *37*, 785−789.
(29) Miehlich, B.; Savin, A.; Stoll, H.; Preuss, H. *Chem. Phys. Lett*. **1989**, *157*, 200−206.
(30) Vosko, S. H.; Wilk, L.; Nusair, M. *Can. J. Phys*. **1980**, *58*, 1200−1211.
(31) The CA names of these LPAH are the following: $C_{34}H_{18}$: anthra[9,1,2-*cde*]benzo[*rst*]penaphene (**1**); benzo[*rst*]phenanthro[10,1,2-*cde*]pentaphene (**2**); tetrabenzo[*a*,*cd*,*j*,*lm*]perylene (**3**); tetrabenzo[*a*,*cd*,*l*-*m*,*o*]perylene (**4**). $C_{38}H_{18}$: anthra[2,1,9,8-*klmno*]naphtho[3,2,1,8,7-*vwxyz*]-hexaphene (**5**); dianthra[2,1,9,8-*stuva*;2′,1′,9′,8′-*hijkl*]pentacene (**6**); dibenzo[*jk*,*uv*]dinaphtho[2,1,8,7-*defg*; 2′,1′,8′,7′-*opqr*]perylene (**7**); diphenanthro[5,4,3-*abcd*;3′,4′,5′-*lmno*]perylene (**8**).
(32) Biedermann, P. U.; Schurig, V.; Agranat, I. *Chirality* **1997**, *9*, 350−353.
(33) Schulman, J. M.; Disch, R. L. *J. Phys. Chem. A* **1997**, *101*, 9176−9179.
(34) Pogodin, S.; Agranat, I. *Org. Lett*. **1999**, *1*, 1387−1390.
(35) Agranat, I.; Suissa, M. R. *Polycycl. Aromat. Compd*. **1992**, *3*, 51−61.

Table 1. Semiempirical Relative Enthalpies of Formation $\Delta\Delta H_f°$ and Ab Initio Relative Energies ΔE_{Tot} (kJ/mol), Selected Semiempirical Enthalpies of Formation $\Delta H_f°$ (kJ/mol) and Ab Initio Total Energies E_{Tot} (Hartree), Ab Initio Enthalpies of Formation ($\Delta H_f°_{(ab\ initio)}$, kJ/mol, at B3LYP/6-31G*), and the Numbers of Kekulé Structures *K* of LPAHs 1−8

		symm	stationary point[a]	AM1 $\Delta\Delta H_f°$	HF/6-31G* ΔE_{Tot}	B3LYP/6-31G* ΔE_{Tot}	B3LYP/6-31G* $\Delta H_f°_{(ab\ initio)}$[b]	*K*
1	**pl**	C_{2v}	GM	652.511[c]	−1298.12044596[d]	−1306.57314759[d]		
1	**pl**	C_{2v}	GM	0.00	0.00	0.00	531.94	41
2	**pl**	C_{2h}	GM	4.01	6.59	3.36	535.31	40
3	**tf**	C_2	GM	7.97	31.08	29.94	558.42	60
3	**a**	C_i	LM	22.96		53.67		
3	**ft**	C_2	SP2	96.68		130.60		
3	**pl**	C_{2h}	SP5	168.31		155.64		
4	**tf**	C_2	GM	6.82	31.66	33.16	561.64	61
4	**s**	C_s	TS	107.08		153.41		
4	**pl**	C_{2v}	SP5	348.70		301.94		
5	**pl**	C_{2v}	GM	746.854[c]	−1449.63141017[d]	−1459.03894157[d]		
5	**pl**	C_{2v}	GM	0.00	0.00	0.00	570.22	52
6	**pl**	C_{2h}	GM	9.58	14.93	8.34	578.56	48
7	**tf**	C_2	GM	−21.47	−4.29	5.47	572.23	96
7	**pl**	C_{2h}	SP3	125.96		119.07		
8	**tf**	C_2	GM	−23.22	−0.18	14.52	581.29	100
8	**pl**	C_{2v}	SP4	304.32		263.18		

[a] At B3LYP/STO-3G; GM − global minimum, LM − local minimum, TS − transition state, SP*n* − saddle point of *n*-th order. [b]Calculated from the respective total energies at B3LYP/6-31G* using the parametrization scheme based on the experimental enthalpies of formation of benzenoid PAHs.[18] [c]Semiempirical enthalpies of formation $\Delta H_f°$ (kJ/mol). [d]Ab initio total energies E_{Tot} (Hartree).

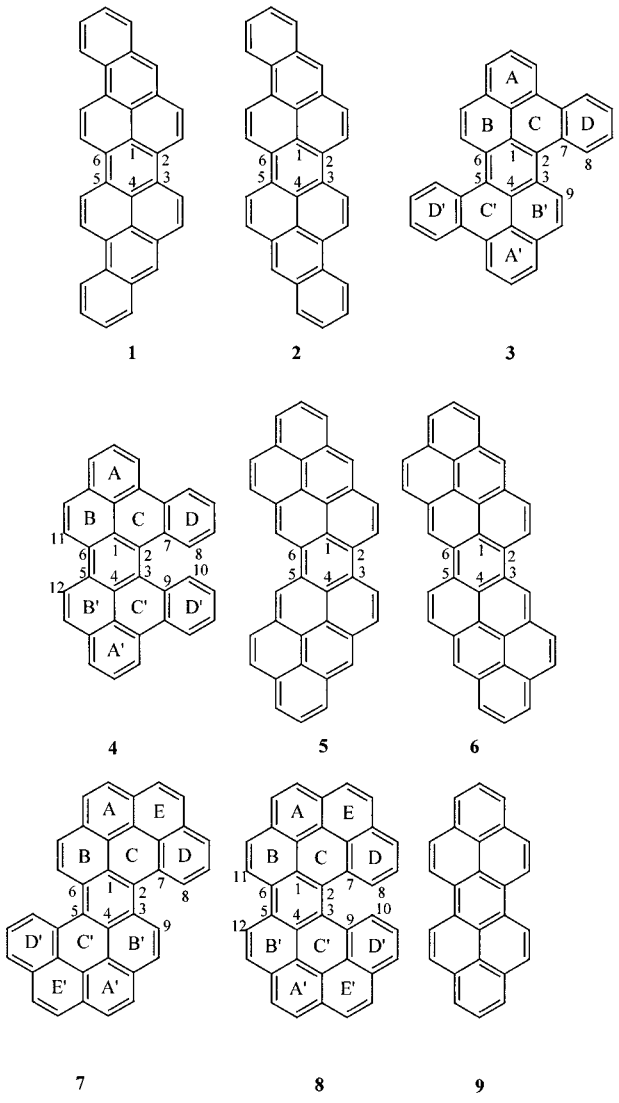

out-of-plane modes are combined, the order is meant to designate the dominant mode. Thus, **ft** is closer to a folded conformation, while **tf** resembles a twisted conformation.

According to B3LYP/6-311G**, the most stable LPAH in the $C_{34}H_{18}$ series was planar C_{2v}-**1**. Its planar C_{2h}-**2** isomer was 3.4 kJ/mol less stable. The corresponding chiral twisted-folded isomers **3** and **4** were significantly less stable than **1**, by 30.4 and 32.3 kJ/mol, respectively. Interestingly, the twisted-folded C_2-**3** with two cove regions was found to be slightly more stable than its corresponding twisted-folded C_2-**4** with one fjord region, ΔE_{Tot} = 3.2 kJ/mol (at B3LYP/6-31G*) and 1.9 kJ/mol (at B3LYP/6-311G**). In the $C_{38}H_{18}$ series, the most stable isomer was planar C_{2v}-**5**. Its planar C_{2h}-**6** isomer was 8.4 kJ/mol less stable. The corresponding chiral twisted-folded isomers C_2-**7** and C_2-**8** were less stable than **5** by 6.4 and 13.8 kJ/mol, respectively. LPAH **tf**-C_2-**7** with two cove regions is significantly more stable than its isomer **tf**-C_2-**8** having one fjord region, ΔE_{Tot} = 7.4 kJ/mol (at B3LYP/6-311G**). Thus, the ab initio DFT calculations, contrary to the semiempirical calculations,[17] predict that one fjord is more destabilizing than two coves in the above LPAHs. Semiempirical calculations also seem to underestimate the destabilization energy in nonplanar LPAH C_2-**7** and C_2-**8**. According to the AM1 and PM3 calculations, the nonplanar chiral $C_{38}H_{18}$ isomers C_2-**7** and C_2-**8** are more stable than their planar isomer C_{2v}-**5** by 21.5 and 23.2 kJ/mol (AM1) and 12.0 and 17.5 kJ/mol (PM3). Herndon's group additivity equation of the MMX $\Delta H_f°$ of planar and nonplanar PAHs, which delineated the energy effects of steric factors causing nonplanarity, including coves and fjords, also predict that two coves are more destabilizing than one fjord.[3a]

It should be noted that in the undecacyclic $C_{38}H_{18}$ series, the energy differences between the planar and the overcrowded isomers are significantly smaller (>50%) than in the nonacyclic $C_{34}H_{18}$ series: E_{Tot}(**pl**-C_{2v}-**5**) − E_{Tot}(**tf**-C_2-**7**) = −6.4 kJ/mol and E_{Tot}(**pl**-C_{2v}-**5**) − E_{Tot}(**tf**-C_2-**8**) = −13.8 kJ/mol, while E_{Tot}(**pl**-C_{2v}-**1**) − E_{Tot}(**tf**-C_2-**3**) = −30.4 kJ/mol and E_{Tot}(**pl**-C_{2v}-**1**) − E_{Tot}(**tf**-C_2-**4**) = −32.3 kJ/mol (at B3LYP/6-311G**). It seems that the steric effect of overcrowding is attenuated in the larger PAHs series and that the relative impact of aromatic stabilization as reflected in the number of Kekulé structures (*K*) is enhanced. In $C_{38}H_{18}$, *K*(nonplanar)/*K*(planar) = 2.0, while in $C_{34}H_{18}$, *K*(nonplanar)/*K*(planar) = 1.5. Within

each series, the differences in K values between planar (C_{2v} versus C_{2h}) isomers and between overcrowded (two coves versus one fjord) isomers is marginal. Another unexpected result is the higher stability of the overcrowded **tf**-C_2-**7** with two coves, relative to the planar C_{2h}-**6**: E_{Tot}(**tf**-C_2-**7**) − E_{Tot}(**pl**-C_{2h}-**6**) = −2.0 kJ/mol. We predict that in larger PAHs series (>C_{38}), overcrowding will not hinder nonplanar isomers from becoming the most stable within a given series.

It is interesting to note that the HF/6-31G* relative energies of **1**−**8** hold an intermediate position between the corresponding semiempirical energies and the DFT B3LYP energies (Table 1). Contrary to the B3LYP/6-31G* results, at HF/6-31G*, the most stable isomer in the $C_{38}H_{18}$ series is twisted-folded C_2-**7**. The planar isomers C_{2v}-**5** and C_{2h}-**6** are 4.3 and 14.9 kJ/mol less stable than **tf**-C_2-**7**. On the other hand, similarly to B3LYP, **tf**-C_2-**7** (with two coves) is more stable than **tf**-C_2-**8** (with one fjord) by 4.1 kJ/mol. In the $C_{34}H_{18}$ series, at HF/6-31G*, the most stable isomer was C_{2v}-**1**. Its planar isomer C_{2h}-**2** was 6.6 kJ/mol less stable. The chiral twisted-folded C_2-**3** and C_2-**4** LPAHs were considerably less stable, 31.1 and 31.7 kJ/mol, respectively. The energy difference between **tf**-C_2-**3** and **tf**-C_2-**4** was only 0.6 kJ/mol.

No experimental heats of formation have been reported for LPAHs **1**−**8**. Using four parameters for the CH group and three different types of carbon atoms in PAHs (derived from the experimental enthalpies of formation of 12 benzenoid PAHs[18]), the heats of formation of compounds **1**−**8** were estimated as shown in Table 1 (at B3LYP/6-31G*).

An attempt was made to estimate the magnitudes of the steric effects causing the overcrowded LPAHs **3**, **4**, **7**, and **8** to deviate from planarity. The geometries of these LPAHs were optimized under the constraints that forced the conformations to remain planar. The resulting energy differences at B3LYP/6-31G* between the twisted-folded C_2 **3**, **4**, **7**, and **8** and their respective planar conformations C_{2h}-**3**, C_{2v}-**4**, C_{2h}-**7**, and C_{2v}-**8** were huge: 125.7, 268.8, 113.6, and 248.7 kJ/mol, respectively. Interestingly, the planar conformations with two coves C_{2h}-**3** and C_{2h}-**7** are considerably less destabilized, relative to the planar conformations C_{2v}-**4** and C_{2v}-**8** with one fjord. However, these energies should be taken with a grain of salt, as these planar conformations are not bona fide minima or transition states but higher order saddle points (SPn, n = 3−5) on the potential energy surfaces. The extreme extent of overcrowding in the planar conformations of **3**, **4**, **7**, and **8** is reflected in the very short nonbonding distances between the bucking hydrogen atoms at the cove regions (137.8 and 138.0 pm in **pl**-C_{2h}-**3** and **pl**-C_{2h}-**7**, respectively) and fjord regions (114.8 and 114.1 pm in **pl**-C_{2v}-**4** and **pl**-C_{2v}-**8**, respectively). The van der Waals radius of hydrogen is 115.5[36] pm, resulting in a van der Waals contact distance of 231 pm. Thus, the above H···H distances in the planar conformations of **3**, **4**, **7**, and **8** reflect about 40% (in **3**, **7**) and 50% (in **4**, **8**) penetration.

The relief of overcrowding in the cove and fjord regions of the nonplanar LPAHs **3**, **4**, **7**, and **8** is reached by twisting of a molecule around the central benzene ring. Another principal mode of deviation from planarity accompanied by a reduction of steric strain is bending of the upper and lower parts of a molecule around the central benzene ring. Depending on the directions of this bending, *anti*-folding and *syn*-folding modes can be distinguished. A search of the conformational spaces of the $C_{34}H_{18}$ LPAHs **3** and **4** revealed an *anti*-folded local minimum **a**-C_i-**3** and a *syn*-folded transition state **s**-C_s-**4**, 23.7 and 120.3 kJ/mol higher in energy than the corresponding global minima **tf**-C_2-**3** and **tf**-C_2-**4**, respectively (at B3LYP/6-31G*). A *syn*-folded-twisted conformation **ft**-C_2-**3** turned out to be a second-order saddle point (at B3LYP/STO-3G). Three-dimensional representations of **tf**-C_2-**3**, **a**-C_i-**3**, **tf**-C_2-**4**, and **s**-C_s-**4** (at B3LYP/6-31G*) are shown in Figure 1 and Figure 2. Fetzer et al. have previously shown that in the case of tetrabenzo[*a*,*cd*,*f*,*lm*]-perylene (**10**), a constitutional isomer of LPAHs **1**−**4** formed in a reductive cross coupling reaction of 13*H*-benzo[*fg*]naphthacen-13-one and phenalenone,[37] a twisted

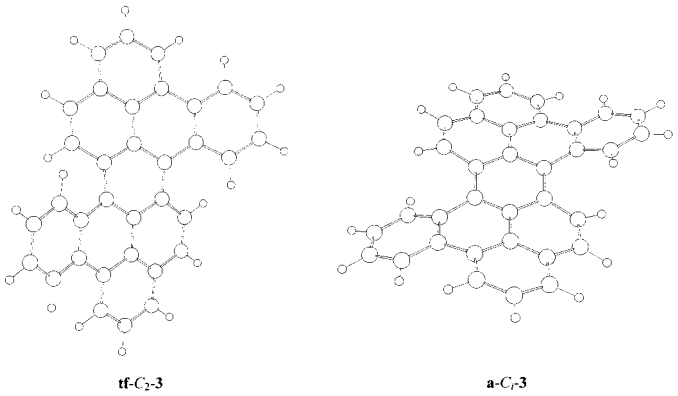

Figure 1. Three-dimensional representation of LPAHs **tf**-C_2-**3** and **a**-C_i-**3** (at B3LYP/6-31G*).

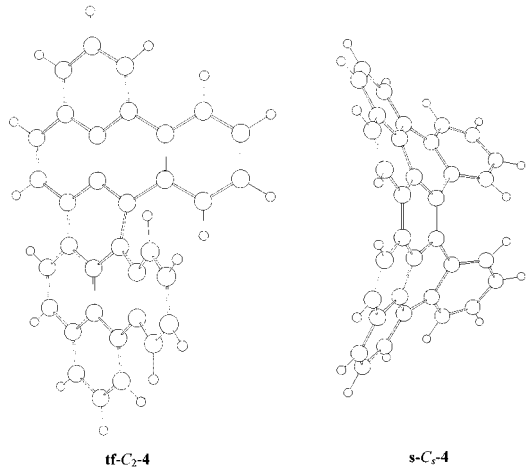

Figure 2. Three-dimensional representation of LPAHs **tf**-C_2-**4** and **s**-C_s-**4** (at B3LYP/6-31G*).

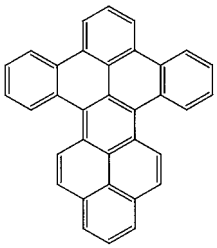

10

(36) Zefirov, Yu. V. *Crystallogr. Rep.* **1997**, *42*, 111−116.

Table 2. Bond Lengths and Nonbonding Distances (pm) at the Central Overcrowded Regions of LPAHs 1−8 and X-ray Molecular Structures of 3 and 7

		symm	distances, pm	AM1	HF/ 6-31G*	B3LYP/ 6-31G*	X-ray[a]	
1	pl	C_{2v}	C^1-C^2	143.2	143.2	143.7		
			C^1-C^6	141.3	140.1	142.4		
			C^2-C^3	139.8	138.7	141.6		
			C^5-C^6	142.6	143.0	143.8		
2	pl	C_{2h}	C^1-C^2	141.9	141.1	142.7		
			C^1-C^6	142.3	141.6	143.1		
			C^2-C^3	141.2	140.8	142.7		
3	tf	C_2	C^1-C^2	141.6	140.5	142.0	141.8	140.7
			C^1-C^6	142.1	141.6	143.3	141.6	142.5
			C^2-C^3	141.3	140.8	142.4	141.6	140.8
			$C^8\cdots C^9$	296.2	301.2	301.0	297.1	294.6
3	a	C_i	C^1-C^2	141.5		142.1		
			C^1-C^6	142.2		143.5		
			C^2-C^3	141.1		142.4		
			$C^8\cdots C^9$	289.4		294.1		
3	ft	C_2	C^1-C^2	141.9		142.8		
			C^1-C^6	142.9		144.3		
			C^2-C^3	141.5		143.4		
			$C^8\cdots C^9$	300.8		303.3		
4	tf	C_2	C^1-C^2	142.9	142.4	143.1		
			C^1-C^6	141.1	140.1	142.3		
			C^2-C^3	140.2	139.5	141.8		
			C^5-C^6	142.3	141.9	142.8		
			$C^8\cdots C^{10}$	286.1	302.4	300.5		
4	s	C_s	C^1-C^2	143.8		144.5		
			C^1-C^6	140.9		141.9		
			C^2-C^3	140.1		143.2		
			C^5-C^6	142.1		142.6		
			$C^8\cdots C^{10}$	288.6		297.2		
5	pl	C_{2v}	C^1-C^2	143.7	144.0	143.9		
			C^1-C^6	141.7	140.8	143.2		
			C^2-C^3	139.1	138.0	141.5		
			C^5-C^6	143.8	144.8	145.2		
6	pl	C_{2h}	C^1-C^2	141.8	141.0	142.5		
			C^1-C^6	142.7	142.4	144.1		
			C^2-C^3	141.4	141.2	143.3		
7	tf	C_2	C^1-C^2	141.7	140.7	142.2	137.8	141.4
			C^1-C^6	142.3	141.9	143.5	141.6	140.7
			C^2-C^3	141.4	141.0	142.6	147.8	143.7
			$C^8\cdots C^9$	296.1	301.4	301.2	301.8	287.8
8	tf	C_2	C^1-C^2	143.6	143.3	143.6		
			C^1-C^6	141.0	139.9	142.3		
			C^2-C^3	139.8	139.1	141.8		
			C^5-C^6	142.9	142.7	143.2		
			$C^8\cdots C^{10}$	283.4	301.6	299.8		

[a] X-ray structure of **3**: ref 40; X-ray structure of **7**: ref 41.

conformer and a folded conformer were revealed.[38] The difference in enthalpy between these two conformers was only 1.7 kJ/mol (at MM2). The existence of two conformers of **10** has also been inferred from infrared absorption and fluorescence spectra.[38]

Table 2 provides bond lengths at the central aromatic ring and contact distances at the central overcrowded regions (cove or fjord) of optimized nonplanar conformations (at AM1, HF/6-31G* and B3LYP/6-31G*) and X-ray molecular structures (where applicable) of LPAHs **1**−**8**. In all the above LPAHs, the bond lengths in the central rings are in the range of the aromatic bond length of graphite, 142.2 pm[39] (at both B3LYP/6-31G* and B3LYP/6-311G**), and bond alternation is relatively small. An exception is **pl**-C_{2v}-**5**, in which the distance $C^2-C^3 = 141.2$ pm and the distance $C^5-C^6 = 145.1$ pm, providing a difference of 3.9 pm (at B3LYP/6-311G**). Ab initio DFT calculations yield bond lengths that are consistently slightly longer than those calculated semiempirically. HF/6-31G* calculated bond lengths are slightly shorter than those calculated semiempirically. The X-ray geometries of **3**[40] and **7**[41] indicated C_1 rather than C_2 conformations, probably due to solid-state effects.[42] Ab initio HF and DFT calculated distances are not in better agreement with the experimental X-ray values than semiempirically calculated ones. However, the reliability of the disordered structure of **7** should be born in the mind. Table 3 gives torsion angles and dihedral angles at the central overcrowded regions of optimized nonplanar conformations

Table 3. The Absolute Values of Torsion and Dihedral Angles at the Central Overcrowded Regions of Semiempirical and ab Initio Optimized Nonplanar Conformations of 3, 4, 7, 8 and of X-ray Molecular Structures of 3 and 7

		symm	angle, deg[a]	AM1	HF/ 6-31G*	B3LYP/ 6-31G*	X-ray data	
3	**tf**	C_2	twist	23.6	23.3	23.7	23.2	22.8
			cove	39.9	41.1	39.9	39.8	40.3
			P1−P2	28.5	30.4	29.6	30.0	
			P3−P4	36.0	38.2	36.9	36.7	
3	**a**	C_I	twist	13.6		15.0		
			cove	32.3		32.2		
			P1−P2	0.00		0.00		
			P3−P4	0.00		0.00		
3	**ft**	C_2	twist	19.7		15.4		
			cove	4.3		4.1		
			P1−P2	46.9		37.8		
			P3−P4	47.9		38.6		
4	**tf**	C_2	twist1	28.1	29.1	30.5		
			twist2	14.6	14.0	14.1		
			fjord	49.3	52.2	51.9		
			P1−P2	19.2	19.4	20.6		
			P3−P4	30.2	31.7	32.2		
4	**s**	C_s	twist1	0.0		0.0		
			twist2	0.0		0.0		
			fjord	0.0		0.0		
			P1−P2	54.1		53.6		
			P3−P4	60.0		58.3		
7	**tf**	C_2	twist	22.6	21.9	22.3	30.4	19.6
			cove	37.1	38.0	37.0	37.8	30.1
			P1−P2	25.1	26.3	26.0	31.0	30.2
			P3−P4	31.1	32.6	31.6	34.7	34.2
8	**tf**	C_2	twist1	25.9	26.7	28.5		
			twist2	15.5	14.7	14.5		
			fjord	46.3	49.1	49.1		
			P1−P2	19.5	19.5	20.7		
			P3−P4	27.4	28.6	29.4		

[a] Torsion angles definitions: twist (**3**) = ($C^7-C^2-C^3-C^9$), twist (**7**) = ($C^7-C^2-C^3-C^9$); twist1 (**4**) = ($C^7-C^2-C^3-C^9$), twist2 (**4**) = ($C^{11}-C^6-C^5-C^{12}$), twist1 (**8**) = ($C^7-C^2-C^3-C^9$), twist2 (**8**) = ($C^{11}-C^6-C^5-C^{12}$); cove (**3**) = ($C^8-C^7-C^3-C^9$), cove (**7**) = ($C^8-C^7-C^3-C^9$); fjord (**4**) = ($C^8-C^2-C^3-C^{10}$), fjord (**8**) = ($C^8-C^2-C^3-C^{10}$); dihedral angles definitions: plane P1 consists of aromatic rings A, B, C, plane P2 consists of aromatic rings A′, B′, C′; plane P3 consists of aromatic rings A, B, C, D, E; plane P4 consists of aromatic rings A′, B′, C′, D′, E′.

(37) Fetzer, J. C.; Biggs, W. R. *Org. Prep. Proced. Int.* **1988**, *20*, 223−230.

(38) (a) Waluk, J.; Fetzer, J.; Hamrock, S. J.; Michl, J. *J. Phys. Chem.* **1991**, *95*, 8660−8663. (b) Morgan, F.; Garrigues, Ph.; Lamotte, M.; Fetzer, J. C. *Polycyclic Aromat. Compd.* **1991**, *2*, 141−153.

(39) Trucano, P.; Chen, R. *Nature* **1975**, *258*, 136−137.

(40) Kohno, Y.; Konno, M.; Saito, Y.; Inokuchi, H. *Acta Crystallogr. B* **1975**, *B31*, 2076−2080.

(41) (a) Robertson, J. M.; Trotter, J. *J. Chem. Soc.* **1959**, 2614−2624. (b) Oonishi, I.; Fujisawa, S.; Aoki, J.; Danno, T. *Bull. Chem. Soc. Jpn.* **1978**, *51*, 2256−2260.

(42) In view of the lack of C_2 symmetry in the X-ray molecular structures of **3** and **7** an attempt was made to calculate the C_1 global minimum conformations of these LPAHs. The B3LYP/STO-3G and B3LYP/6-31G* optimizations of **3** and **7** yielded C_1 conformations characterized by slightly higher total energies than the respective C_2 conformations ($E_{Tot}(C_1$-**3**$) - E_{Tot}(C_2$-**3**$) = 0.039$ kJ/mol, $E_{Tot}(C_1$-**7**$) - E_{Tot}(C_2$-**7**$) = 0.040$ kJ/mol at B3LYP/6-31G*), while the geometries of the respective C_1 and C_2 conformations were essentially identical.

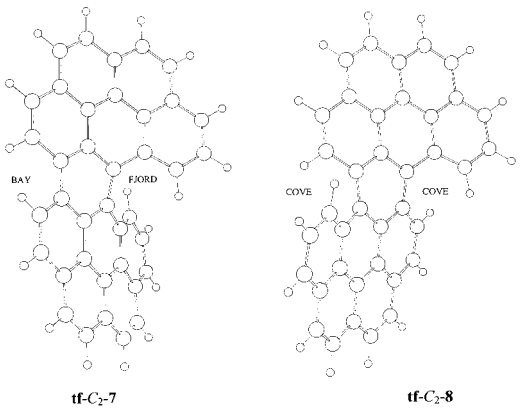

Figure 3. Three-dimensional representation of LPAHs **tf**-C_2-**7**and **tf**-C_2-**8** (at B3LYP/6-311G**).

(at AM1, HF/6-31G*, and B3LYP/6-31G*) and X-ray molecular structures of LPAHs **3**, **4**, **7**, and **8**. In the undecacyclic $C_{38}H_{18}$ series, the cove and fjord torsion angles at the central overcrowded regions are smaller than in the nonacyclic $C_{34}H_{18}$ series: 37.4° (**tf**-C_2-**7**, cove) and 49.4° (**tf**-C_2-**8**, fjord) vs 40.4° (**tf**-C_2-**3**, cove) and 52.1° (**tf**-C_2-**4**, fjord) (at B3LYP/6-311G**). The values of the dihedral angles between P3−P4 planes are also decreasing: 32.1° (**tf**-C_2-**7**) and 29.4° (**tf**-C_2-**8**) vs 37.4° (**tf**-C_2-**3**) and 32.1° (**tf**-C_2-**4**) (at B3LYP/6-311G**). It is noted that the local nonplanarity reflected in the large values of the torsion angles at the overcrowded regions is quite high for twisted-folded conformations of LPAHs **3**, **4**, **7**, and **8**, while the dihedral angles describing the overall geometry are smaller. Both B3LYP/6-31G* and B3LYP/6-311G** calculated torsion and dihedral angles are usually larger than the respective semiempirically calculated ones and are better correlated with the experimentally determined X-ray values. The three-dimensional representation of optimized global minima conformations of **tf**-C_2-**7** and **tf**-C_2-**8** (at B3LYP/6-311G**) is shown in Figure 3. The nonbonding distances between the pairs of carbon atoms C^8 and C^9 at the cove regions of **tf**-C_2-**3** and **tf**-C_2-**7** are 301.2 and 301.4 pm, respectively (at B3LYP/6-311G**). The nonbonding distances between C^8 and C^{10} at the fjord regions of **tf**-C_2-**4** and **tf**-C_2-**8** are 300.7, 300.2 pm, respectively (at B3LYP/6-311G**). These distances are smaller than the sum of the van der Waals radii of two carbon atoms (342 pm[36]). The nonbonding distances between the carbon atoms at cove and fjord regions are almost identical, reflecting similar degree of overcrowding.

Generally, the B3LYP/6-311G** relative energies as well as geometries were not significantly different from the corresponding B3LYP/6-31G* relative energies and geometries, and the upgrade from the 6-31G* to the 6-311G** basis set does not seem to be critical, unless high accuracy is desired.

In conclusion, the ab initio DFT calculations, contrary to the former semiempirical calculations, predict that two coves have a less destabilizing effect than one fjord in the LPAHs **1**−**8**. In addition, the destabilization energies in overcrowded LPAHs are decreasing with the increase of the number of benzene rings.

Acknowledgment. We thank a reviewer for drawing our attention to the existence of two conformations of LPAH **10** with very similar energies.

Supporting Information Available: Table S1 contains the ab initio HF/STO-3G, HF/6-31G*, B3LYP/STO-3G, B3LYP/6-31G*, and B3LYP/6-311G** total energies and semiempirical AM1 and PM3 enthalpies of formation of LPAHs **1**−**8**. Table S2 contains the ab initio HF/STO-3G, HF/6-31G*, B3LYP/STO-3G, B3LYP/6-31G*, and B3LYP/6-311G** relative energies and semiempirical AM1 and PM3 relative enthalpies of formation of LPAHs **1**−**8**. Table S3 contains bond lengths and nonbonding distances at the central aromatic ring of optimized conformations of LPAHs **1**−**8** and X-ray molecular structures of **3** and **7** (at AM1, PM3, HF/STO-3G, HF/6-31G*, B3LYP/STO-3G, B3LYP/6-31G*, and B3LYP/6-311G**). Table S4 contains torsion angles and dihedral angles at the central overcrowded regions of optimized nonplanar conformations (at AM1, PM3, HF/STO-3G, HF/6-31G*, B3LYP/STO-3G, B3LYP/6-31G*, and B3LYP/6-311G**) and X-ray molecular structures of LPAHs **3**, **4**, **7**, and **8**. Tables S5−S19 contain the optimized geometries of the studied conformations of LPAHs **1**−**8** (as Cartesian coordinates).

JO0107251